universe

MDPI

Article

Implications of the Unique Active Galaxy 4C +55.17 for the Issues of Cosmology

Vera G. Sinitsyna * and Vera Y. Sinitsyna

P.N. Lebedev Physical Institute, Russian Academy of Science, Moscow 119991, Russia; sinicinavy@lebedev.ru
* Correspondence: sinits@sci.lebedev.ru

Abstract

Extragalactic background light (EBL), formed by the light radiated and re-radiated by stars, galaxies, and active galactic nuclei throughout the evolution of the Universe, brings the imprint of the history of the rate of the formation of emitting astrophysical objects and the Universe's expansion. It makes EBL one of the fundamental quantities in cosmology. The optical depth for high-energy emission from the distant active galactic nuclei provides a constraint for the EBL density that is clear from the foreground galactic and other emissions, and, therefore, for the cosmological parameters. In this work, we investigate the high-redshift active galaxy 4C +55.17 (z = 0.902), whose unusually hard and stable high-energy spectrum makes it a valuable probe of EBL-induced absorption effects. Using observations extending from GeV to TeV energies, we reconstruct the optical depth associated with gamma-ray propagation and compare the inferred attenuation with predictions from existing EBL models. The results favor relatively low EBL intensities in the optical and infrared bands, consistent with low-level EBL models and suggesting reduced star formation activity and dust contributions over cosmic evolution. We further explore the cosmological implications of the reconstructed optical depth and derive constraints on the Hubble constant in the range $H_0 \approx 64$–74 km s^{-1} Mpc^{-1}, with an average value of $H_0 = 69 \pm 4$ km s^{-1} Mpc^{-1}. These findings demonstrate the potential of hard-spectrum, high-redshift gamma-ray sources such as 4C +55.17 as cosmological probes for studying EBL evolution and addressing current tensions in cosmological parameter measurements.

Keywords: active galactic nuclei; 4C +55.17; gamma-rays; cosmic background radiation; extragalactic background light; cosmology

Check for updates

Academic Editors: Hermano Velten, Panayiotis Stavrinos, Antonino Del Popolo, Tina Kahniashvili, Jean-Michel Alimi and Yi-Fu Cai

Received: 28 March 2026
Revised: 22 May 2026
Accepted: 27 May 2026
Published: 30 May 2026

Copyright: © 2026 by the authors. Licensee MDPI, Basel, Switzerland. This article is an open access article distributed under the terms and conditions of the Creative Commons Attribution (CC BY) license.

1. Introduction

The evolution of the Universe is seen through light that was emitted by the objects at different cosmological epochs. The earliest sights of the Universe's history viewed as relic radiation are related to the times of the epoch of recombination and observed in the mm wavelength range as an intense emission called the cosmic microwave background (CMB). The later epochs of radiation history after the "Dark Ages" are collected in the extragalactic background light (EBL). Since the first stars and then galaxies, active galactic nuclei and other large-scale structures started to form after the epoch of reionization; their emission in the ultraviolet and optical wavelengths that has accumulated up to now fills the Universe. This light is the cosmic optical background (COB) that covers the 0.1–8 μm range. The cosmic infrared background component at the 8–1000 μm wavelengths is formed by the emission from the dust filling the interstellar medium and the vicinity of the large-scale objects, which re-radiates the absorbed starlight. These components, between

0.1 and 1000 μm, are both parts of the extragalactic background light, carrying the history of the radiation in the Universe, and their knowledge is of high importance for the models of the formation and evolution of stars and galaxies (see, for example, [1–3]). The dependence of the EBL density on the history of the expansion of the Universe, implying cosmology-dependence, makes EBL an instrument for the measurement of the Hubble constant H_0. It should be noted here that there is about 3σ tension in the Hubble constant determined from the observations of the cosmic microwave background radiation by Planck [4] and from those of the detections of Ia-type supernovae with distance calibration from Cepheid variable stars [5,6]. Thus, the determination of H_0 with a method based on the knowledge of the EBL density can serve for the resolving of this Hubble tension [7,8]. Many observational efforts have been made to measure EBL photon intensity. However, direct observations are highly contaminated by foregrounds of the zodiacal light (e.g, [9,10]) and Galactic emission (e.g, [11–16]), which results in the overestimation of the intensity of the EBL. Measurements based on the integration of the light produced by galaxies [17–19], which were resolved in the deep surveys, can give lower limits on the EBL, but this method does not take into account unresolved sources.

The constraints on the intensity of the extragalactic background light can be implemented by means of the indirect approach using the observations of distant active galactic nuclei (AGN) in high and very high energies [2,3,20]. The propagation of gamma-rays from AGNi is accompanied by absorption by the field of EBL photons, which imprints on the spectra of these distant sources. The underlying process is the electron–positron pair creation in the interaction of high-energy gamma-rays from distant extragalactic sources with the EBL photon field that was described by [21,22]. The annihilation process leads to the attenuation of the spectra of gamma-rays from AGNi, which is seen as an exponential cutoff if measured in the GeV-TeV energy range. This gamma-ray opacity can be characterized by an optical depth depending on the redshift of the observed source and on the gamma-ray energy, as well as on the density of EBL photons, which is in turn cosmology-dependent, as it depends on the history of the formation of the emitting objects and expansion. So, the observations of distant AGNi at high and very high energies allow us to measure the Universe expansion rate, known as the Hubble constant, place limits on the EBL density [20], and also lead to the derivation of the parameters of the models of the formation and evolution of stars and galaxies.

Active galactic nuclei of the blazar class are known to be bright in high- and very-high-energy gamma-rays. The extraordinary power of blazars comes from the relativistic jets launched by the black hole engine in the centers of AGNi. The blazar class of AGNi includes BL Lacertae (BL Lac) objects and flat-spectrum radio-loud quasars (FSRQs). These two subclasses of blazars also exhibit a difference not only in the features of the continuum spectrum, but also in gamma-ray properties [23,24]. FSRQ objects are more luminous and higher redshifted objects than BL Lac ones, but usually have a softer spectral index. As seen in the Fermi LAT 4th AGN Catalogue, the redshift distribution of BL Lacs peaks at $z < 0.5$, whereas the FSRQ one peaks at $z \sim 1.2$ [23,24]. The method of constraining the EBL density using the observations of gamma-rays from AGNi has a difficulty, which is the uncertainty in the initial, unabsorbed spectrum of AGNi. If the AGN lies at a distance, implying the high-energy part of the observed spectrum is strongly influenced by the EBL photon field, it would be preferable if the object itself did not have an unexpected curvature of the spectrum, and the lower energy part should be known. The pair-production cross-section shape makes the UV–Optical–IR range of EBL sensitive to the GeV-TeV gamma-rays from AGNi at redshifts of $z \sim 1$. Thus, the observations of the powerful FSRQs with a hard spectrum in the GeV-TeV energy range can serve as cosmological probes of the extragalactic background light.

https://doi.org/10.3390/universe12060161

2. 4C +55.17 Viewed in Gamma-Rays

4C +55.17 is a high-redshifted radio-loud blazar which was classified as a flat-spectrum radio quasar [25]. The object's redshift is z = 0.896 [25,26], but it was later determined as z = 0.902 [27]. It should be noted that the revision of the categorization of this object as an FSRQ was considered to explain its features, which are peculiar to the FSRQ type of quasars [28,29]. In comparison with FSRQs, 4C +55.17 demonstrates none of the blazars' characteristics such as a central compact radio core, highly variable fluxes of emission in the wide energy range, high brightness temperatures, etc. [28–30]. Thus, due to its morphological and spectroscopic properties in radio and optical ranges, it was suggested that 4C +55.17 belongs to the class of compact symmetric objects (see [31] for a review, and [28]). High-energy gamma-ray emission with the high-level flux of $(9.1 \pm 1.6) \times 10^{-8}$ ph cm^{-2} s^{-1} corresponding to a luminosity of the order of $L_\gamma \sim 10^{47}$ erg s^{-1} from the 4C +55.17 was detected first by EGRET at energies of $E > 100$ MeV [32,33]. Such a flux value was recognized as high among the sources detected and then deeply studied by the EGRET telescope [33].

In the energy range of 100 MeV–1 TeV, 4C +55.17 was detected by Fermi LAT [34] as a very bright source of gamma-rays with a hard power-law spectrum with $\Gamma \sim -2.04$ [35,36]. Also, during the entire period of observations since 2008, 4C +55.17 was found to be a low-variable object with a variability index lying in the range of $p = 23.4 \div 32.58$ [35–37] (where a variability index is defined in Section 3.6 of [37], a value $p > 41.64$ identifies a variable source at a 99% confidence level). Due to the characteristics of 4C +55.17 detected by Fermi LAT at high energies, this object was recognized as a promising high-redshift candidate for the source of the very-high-energy emission.

So, the detection of emission from 4C +55.17 by Fermi LAT from 100 MeV up to 1 TeV motivated us to start the observations of this object by the SHALON experiment [38–40] in a very-high-energy range at >800 GeV. Intensive observations were carried out with the SHALON telescope in the periods 2012–2016 and 2024–2026. 4C +55.17 was detected at energies of >800 GeV by SHALON [41] with a statistical significance of 10.7σ (evaluated according to the Li&Ma method [42]). The average integral flux of $(0.67 \pm 0.09) \times 10^{-12}$ cm^{-2} s^{-1} was determined throughout the entire observations. A power law with exponential cutoff in the form of $dF/dE = N_0 \times (E/\mathrm{TeV})^{k_\gamma} \times exp(-E/E_{cutoff})$ can well fit the points of the observed energy spectrum of 4C +55.17 in the energy range 0.8–10 TeV, with the photon index of $k_\gamma = -2.2 \pm 0.23$ and $E_{cutoff} = 5.4 \pm 1.7$ with ($\chi^2 = 1.2$ at DoF = 4). Figure 1 shows the high- and very-high-energy gamma-ray spectra of 4C +55.17. The points are the experimental data from Fermi LAT and SHALON observations; the dashed lines are the fits to the observed spectra.

The data about 4C +55.17 intensity were taken with the SHALON telescope in the different years of the long period from 2012 to 2026. The average integral flux of TeV gamma-rays is presented above. However, during the long-term observations, no evidence of variation in the intensity of emission from 4C +55.17 at very high energies was found [43], as there were no significant changes in the flux detected. Given the high redshift of 4C +55.17, it should be taken into account that its intrinsic spectrum of very-high-energy gamma-rays is strongly modified by the interaction with photons of extragalactic background light [21,22]. Depending on the applied model of the EBL intensity [44–50], for the redshift of 4C +55.17, the energy of the spectrum cutoff associated with the EBL absorption lies in the range of 62–195 GeV. In order to explain the observed spectrum of 4C +55.17 at the whole energy range from 100 MeV to 10 TeV, a much lower density of EBL should be assumed compared to the baseline model from [44,45,50], which overpredicts the level of EBL, leading to the unbounded exponential spectral rise at the highest energies (see Figure 1's gray area). For further analysis, the object spectrum described by the Log-Parabola shape $dF/dE \sim (E/E_0)^{(\alpha - \beta' \log(E/E_0))}$ with $\alpha = -2.01 \pm 0.53$ and $\beta' = 0.05 \pm 0.012$ should be

assumed. This spectrum is presented in Figure 1 with a red line. It is an extension of the Fermi LAT data points in the range 50 MeV–10 GeV prior to the energy of the model-expected cutoff due to the EBL attenuation, and can be accepted as an intrinsic spectrum of the object.

3. Optical Depth Dependence on Cosmology

Opacity to the high-energy gamma-rays, which occurs due to the pair production in the interactions between a gamma-ray and a photon of EBL, is characterized by a gamma-ray optical depth τ and can be analytically given by

$$\tau(E_0, z_0) = \int_0^{z_0} \frac{dL}{dz}\, dz \int_{-1}^{1} \frac{1-\mu}{2}\, d\mu \int_{\epsilon_{th}}^{\infty} n(\epsilon, z)\, \sigma_{\gamma\gamma}(E, \epsilon, z, \mu)\, d\epsilon \tag{1}$$

where E_0 is the observed energy and z_0 is the redshift of the source of gamma-rays. The threshold energy of the interaction leading to the pair production is given by the lower limit of the energy integral ϵ_{th}

$$\epsilon_{th} \equiv \frac{2m_e^2 c^4}{E\mu} \tag{2}$$

where E is the gamma-ray energy and ϵ is the energy of the EBL photon (both of these energies are taken in the rest-frame at redshift z), and $\mu = 1 - \cos\theta$, with θ being the angle of the interaction of the gamma-ray and EBL photon. The constant m_e is the mass of an electron, and c is the speed of light. Equation (1) includes the factor $n(\epsilon, z)$, which is the EBL photon density per unit of photon energy, and $\sigma_{\gamma\gamma}(E, \epsilon, z, \mu)$ is the cross-section of photon–photon pair production, and whose dependence on E, ϵ, z, and μ can be written through the dependent on the value ϵ_{th} from Equation (2), factor β, which is given by

$$\beta \equiv \frac{\epsilon_{th}}{\epsilon(1+z)^2} \tag{3}$$

Given factor β from Equation (3), the cross-section of photon–photon pair production $\sigma_{\gamma\gamma}(E, \epsilon, z, \mu)$ can be written as

$$\sigma_{\gamma\gamma}(E, \epsilon, z, \mu) = \frac{3\sigma_T}{16}(1-\beta^2)[-4\beta + 2\beta^3 + (3-\beta^4)\ln\frac{1+\beta}{1-\beta}] \tag{4}$$

Equation (1) shows a distance element dL/dz, defining the variation of the space element with redshift. The standard Friedmann–Lemaitre–Robertson–Walker metric is

$$\frac{dL}{dz} \equiv c\frac{dt}{dz} = \frac{c}{H_0}\frac{1}{(1+z)}\frac{1}{\sqrt{(\Omega_\Lambda + \Omega_M(1+z)^3)}} \tag{5}$$

where the Hubble constant H_0, matter density Ω_M, and dark energy density Ω_Λ are the parameters of the flat ΛCDM cosmology [51], implying $\Omega_\Lambda = 1 - \Omega_M$, which is validated by observations, including the cosmic microwave background anisotropies measured by Planck. It should be noted that the values of H_0 and Ω_M can lie in the range of $40 < H_0 < 95$ km s^{-1} Mpc^{-1} and $0.05 < \Omega_M < 0.6$, which is in agreement with independent observational constraints. As can be seen from Equation (1), the optical depth τ is dependent on cosmological parameters through the EBL density evolution $n(e, z)$ and through the distance element from Equation (5) presenting the propagation of the extragalactic gamma-ray through the Universe.

4. Implications of 4C +55.17 for the EBL Study

Since 4C +55.17 is the extragalactic object with the high redshift of z = 0.902, its spectrum at high energies is strongly modified by the interaction of TeV gamma-rays with photons of EBL. For the case of 4C +55.17, the energy of cutoff caused by the EBL absorption lies in the range of several tens of GeV [44,46–50]. It means that the Fermi LAT measured spectrum at energies below this value is supposed to be unabsorbed and is an intrinsic spectrum of the source (see Section 2). Also, the features of 4C +55.17 that are unusual for an FSRQ object, namely a hard spectrum in the GeV energy range together with the absence of variation in the high and very-high energy flux, which suggests no significant changes in the source spectrum, make the determination of the intrinsic spectrum at energies of >800 GeV up to several TeVs, by extrapolation to higher energies, possible.

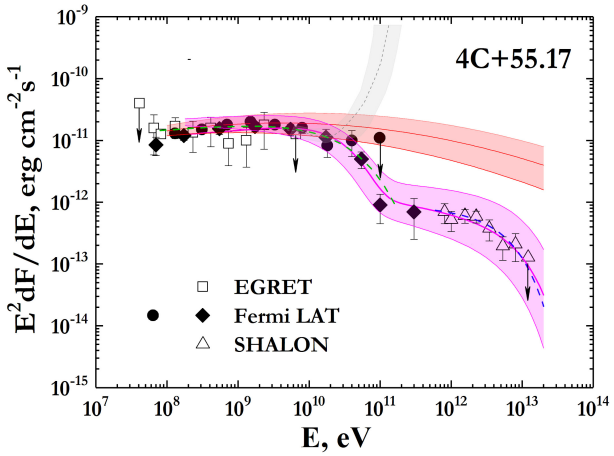


Figure 1. Spectral energy distribution of 4C +55.17: The points correspond to the long-term experimental data from Fermi LAT [35,36] and SHALON observations. △ at TeV energies show the data from SHALON experiment. The dashed green and blue lines are the fits to the observed data points. The red line and area is an assumed intrinsic spectrum of 4C +55.17. The magenta line and area present the spectrum fit to the intrinsic spectrum with attenuation due to the optical depth from Figure 2, light-red area. The gray area and dashed gray line show the de-absorbed spectrum of 4C +55.17 using the [44] model.

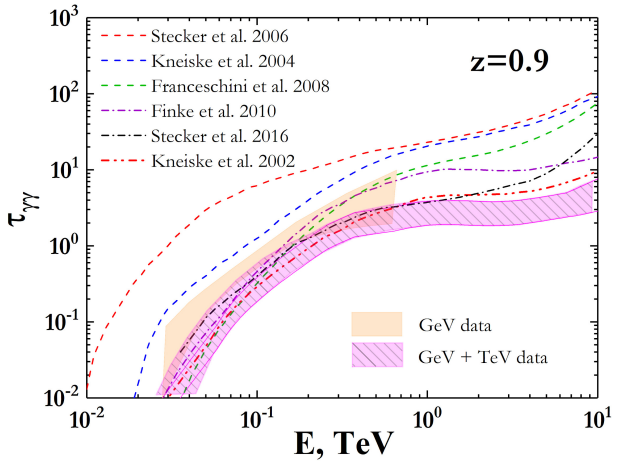


Figure 2. Optical depth $\tau_{\gamma\gamma}$ for several EBL models at z = 0.9 and from the measurements. The baseline model from [44], dashed red line; the model of [45], dashed blue line; the model of [50], dashed green curve; the model of [49], dot-dashed violet curve; the model independent results of [46], dot-dashed black line; and the model with weak infrared output from [47], dot-dot-dashed red curve. The measurements of the opacity $\tau_{\gamma\gamma}$ from the Fermi data [52,53] (light-orange area) and from SHALON observations (magenta dashed area).

For the 4C +55.17 object, a Log-Parabola intrinsic spectrum shape was assumed to describe the unabsorbed, or weakly EBL-influenced, part of the high-energy spectrum in the form of $dF/dE = K \times (E/E_0)^{(\alpha - \beta' \log(E/E_0))}$, where $K = (1.2 \pm 0.43) \times 10^{-12}$ is the flux normalization at $E_0 = (4 \pm 0.8) \times 10^9$ eV energy, $\alpha = -2.01 \pm 0.53$ is the spectral index, and the curvature $\beta' = 0.05 \pm 0.012$. The absorption by EBL photons is described by a modification term $e^{-\tau(E,z)}$, where $\tau(E,z)$ is the optical depth depending on the photon energy E and source redshift z. Then, the observed spectrum can be given by $F_{obs}(E) = F_{intric}(E) \times e^{-\tau(E,z)}$ where $F(E)_{obs}$ is the 4C+55.17 spectrum observed in the experiment. The value $\tau(E,z)$ can be defined through modified models' quantities as $\tau(E,z) = b(E) \times \tau_{mod}(E,z)$, where $\tau_{mod}(E,z)$ is the optical depth predicted by different EBL models [46–50] and $b(E)$ is a scaling parameter. Thus, the EBL optical depth, predicted by different models, can be scaled to fit the observed data. As a result, the level of absorption with EBL can be investigated, together with estimations of cosmological constants.

The optical depth reconstructed from the observations of 4C +55.17 in the wide energy range from MeV up to TeV is presented in Figure 2 together with that calculated within the models of EBL density [44,46–50]. *In* the considered energy range from GeV and higher, up to TeVs, gamma-rays observed by experiments at Earth and coming from the objects at redshift of z = 0.902 interact mostly with optical and infrared photons of 1–100 μm. In the range spanning from UV to the optical part of the cosmic background, those models based on resolved galaxy counts [46–50] and predicting a minimal EBL density are found to well describe the Fermi LAT data and extension to the lowest-energy part of the TeV spectrum of 4C +55.17. The optical depth obtained in [52,53] from the observation of active galactic nuclei at z $\sim$ 0.9 by Fermi LAT is presented in Figure 2 (orange area) together with one for 4C +55.17 (Figure 2, magenta area). Those models that assume a larger EBL intensity in the UV and optical ranges would produce a stronger attenuation of the gamma-ray signal than observed in both Fermi LAT and SHALON experiments (see Figure 2, gray area). Considering the optical to near infrared range of EBL, the spectrum detected up to 5 TeV corresponds to the gamma-ray attenuation imposed by the low-level values of EBL density predicted in [54,55] and also extracted from observations by Fermi LAT [53]. It leads to the low star formation rate at the considered redshift as predicted at the low band of the models [46–48,56]. The level of gamma-ray emission described by the spectrum at >5 TeV points to the very low values of cosmic infrared background up to far infrared range below (within 30–40%) of ones predicted by [47,48] models, which suggest a low amount of dust in the star formation regions through the evolution of the radiation expanding across the metagalaxy.

Referring back to the observational data: considering the optical depth extracted from the scaled models, and assuming the intrinsic spectrum shown in Figure 1 with the red line and light-red area, the attenuated spectrum of 4C +55.17 at high and very-high energies is calculated. It is presented in Figure 1 with a magenta line and light-magenta area. The calculated attenuated spectrum well fits the data points at high and very-high energies obtained in observations of 4C +55.17 by Fermi LAT and SHALON. The resulting de-absorbed, intrinsic spectrum of 4C +55.17 extracted in the assumption of the EBL density scaled from the models and leading to the optical depth from Figure 2 can be described by the shape in the form presented in Figure 1 by the light-red area. Particularly important is that the predicted shape of the intrinsic spectrum of 4C +55.17 is an extension of the Fermi LAT data points, whose features include the spectral fall at the TeV energies, with the intensity of the Inverse Compton peak having the value observed by Fermi LAT, and lying in the GeV energy range [23,24,29].

It was noted above that there is inconsistency between the Hubble constant determined from the Planck observations of the CMB temperature and polarization anisotropies

and those from measurements of Cepheids and Type Ia supernovae. The Planck Collaboration estimation from the measurements at the cosmological distances gives the value $H_0 = 67.4 \pm 0.5$ km s^{-1} Mpc $^{-1}$ [4], whereas the value from local measurements of supernovae is $H_0 = 73.2 \pm 1.3$ km s^{-1} Mpc^{-1} [5,6]. As proposed in [20] and mentioned above, the knowledge of the EBL density during the observations of spectra of distant quasars in the energy range from GeV to TeV can be used as a method for constraining the Universe's expansion rate. The EBL optical depth extracted through those observations is proportional to the distance traveled by gamma-rays from their source to the Earth, which in turn is inversely proportional to H_0 (see Equations (1), (3), (4) and (5)). Having the optical depth determined, for the distant source, the H_0 can be directly estimated.

For the estimation of H_0 from observations of spectra of AGNi at high energies, the cosmological parameter Ω_M was fixed at a value of 0.32 to follow the Planck cosmology. Then the value of H_0 was varied to match the optical depth extracted from observations. In Figure 2, the magenta area presents the optical depth obtained for the 4C +55.17 with the Hubble constant lying in the range 64–74 km s^{-1} Mpc^{-1}, with the average value $H_0 = 69 \pm 4$ km s^{-1} Mpc^{-1}. The lower value of H_0 requires the higher scaling of the models to the lower levels of the EBL density. The larger value corresponds to the optical depth obtained under assumptions of EBL density values closer (within the 25%) to the models' ones [46–49]. The average value of H_0 revealed from observations of only one hard high-energy spectrum AGN object 4C +55.17 is consistent with the one obtained from the Type Ia supernovae measurements within the local universe, as well as with the values from the probes of the CMB at cosmological distances. The collection of observation data from more samples of distant hard-high-energy spectrum active galactic nuclei will clarify both the parameters of the EBL models and the evolutionary models.

5. Conclusions

The investigations of the high- and very-high-energy properties of the distant and powerful active galactic nuclei of the blazar class, having a hard spectrum, give a unique instrument for the study of the level of extragalactic background light, and also the cosmological constants. The most promising are specifically those high-redshifted blazar-type objects characterized by the absence of significant flux variability, but as powerful as FSRQs, having a hard spectrum, with a spectral energy distribution high-energy part peaking in the GeV-TeV range. These features, being unusual for both BLLacs and FSRQs, make it possible, first, to detect these objects up to very high energies, and then to more reliably assume the intrinsic spectrum of the distant object for the further reconstruction of the EBL density. Observations of an unusual quasar 4C +55.17 at z = 0.902, having a very hard spectrum as observed by Fermi LAT and extended up to TeV energies, were used for the estimation of the level of the EBL density in the optical to infrared band. The measured density of the optical part of EBL is consistent with the values obtained within the low-level intensity models [46–50] and ones extracted from the Fermi LAT observations [53], which points to the low star formation rate [56]. The values of the density of the infrared part of the EBL that were measured from the TeV gamma-ray spectrum correspond to models that assume a low contribution of dust in the star formation regions [47,48]. Cosmological measurements based on the attenuation of gamma-rays impose constraints on the Hubble constant lying in the range corresponding to the values obtained in both the local and cosmological distances. Further searches and detections of the sources of gamma-rays having unusual properties similar to 4C +55.17 will serve to study the high-redshift universe at high and very high energies, in particular, the fits of the level of extragalactic background light, leading to the estimation of the star formation rate and resolving the Hubble tension.

https://doi.org/10.3390/universe12060161

Author Contributions: All authors contributed equally. All authors have read and agreed to the published version of the manuscript.

Funding: This research received no external funding.

Data Availability Statement: The original contributions presented in this study are included in the article. Further inquiries can be directed to the corresponding author.

Conflicts of Interest: The authors declare no conflict of interest.

References

1. Dwek, E.; Arendt, R.G.; Hauser, M.G.; Fixsen, D. The COBE Diffuse Infrared Background Experiment Search for the Cosmic Infrared Background. IV. Cosmological Implications. *Astrophys. J.* **1998**, *508*, 106. [CrossRef] [PubMed]
2. Primack, J.R.; Bullock, J.S.; Somerville, R.S.; MacMinn, D. Probing Galaxy Formation with TeV Gamma Ray Absorption. *Astropart. Phys.* **1999**, *11*, 93. [CrossRef]
3. Dwek, E.; Slavin, J. On the Determination of the Cosmic Infrared Background Radiation from the High-Energy Spectrum of Extragalactic Gamma-Ray Sources. *Astrophys. J.* **1994**, *436*, 696. [CrossRef]
4. Aghanim, N.; Akrami, Y.; Ashdown, M.; Aumont, J.; Baccigalupi, C.; Ballardini, M.; Banday, A.J.; Barreiro, R.B.; Bartolo, N.; Basak, S.; et al. Planck 2018 results. VI. Cosmological parameters. *Astron. Astrophys.* **2020**, *641*, A6. Erratum in *Astron. Astrophys.* **2021**, *652*, C4.
5. Riess, A.G.; Casertano, S.; Yuan, W.; Macri, L.; Bucciarelli, B.; Lattanzi, M.G.; MacKenty, J.W.; Bowers, J.B.; Zheng, W.; Filippenko, A.V.; et al. Milky Way Cepheid Standards for Measuring Cosmic Distances and Application to Gaia DR2: Implications for the Hubble Constant. *Astrophys. J.* **2018**, *861*, 126. [CrossRef]
6. Riess, A.G.; Casertano, S.; Yuan, W.; Bowers, J.B.; Macri, L.; Zinn, J.C.; Scolnic, D. Cosmic Distances Calibrated to 1% Precision with Gaia EDR3 Parallaxes and Hubble Space Telescope Photometry of 75 Milky Way Cepheids Confirm Tension with ΛCDM. *Astrophys. J. Lett.* **2021**, *908*, L6. [CrossRef]
7. Salamon, M.H.; Stecker, F.W.; de Jager, O.C. A New Method for Determining the Hubble Constant from Sub-TeV Gamma-Ray Observations. *Astrophys. J. Lett.* **1994**, *423*, L1. [CrossRef]
8. Mannheim, K.; Westerhoff, S.; Meyer, H.; Fink, H.H. Beacons at the gamma ray horizon. *Astron. Astrophys.* **1996**, *315*, 77.
9. Wright, E.L. DIRBE minus 2MASS: Confirming the Cosmic Infrared Background at 2.2 Microns. *Astrophys. J.* **2001**, *553*, 538. [CrossRef]
10. Korngut, P.M.; Kim, M.G.; Arai, T.; Bangale, P.; Bock, J.; Cooray, A.; Cheng, Y.T.; Feder, R.; Hristov, V.; Lanz, A.; et al. Inferred Measurements of the Zodiacal Light Absolute Intensity through Fraunhofer Absorption Line Spectroscopy with CIBER. *Astrophys. J.* **2022**, *926*, 133. [CrossRef]
11. Toller, G.N. The extragalactic background light at 4400 Å. *Astrophys. J. Lett.* **1983**, *266*, L79. [CrossRef]
12. Hauser, M.G.; Arendt, R.G.; Kelsall, T.; Dwek, E.; Odegard, N.; Weiland, J.L.; Freudenreich, H.T.; Reach, W.T.; Silverberg, R.F.; Moseley, S.H.; et al. The COBE Diffuse Infrared Background Experiment Search for the Cosmic Infrared Background. I. Limits and Detections. *Astrophys. J.* **1998**, *508*, 25. [CrossRef]
13. Bernstein, R.A.; Freedman, W.L.; Madore, B.F. The First Detections of the Extragalactic Background Light at 3000, 5500, and 8000 Å. I. Results. *Astrophys. J.* **2002**, *571*, 56. [CrossRef]
14. Matsuoka, Y.; Ienaka, N.; Kawara, K.; Oyabu, S. Cosmic Optical Background: The View from Pioneer 10/11. *Astrophys. J.* **2011**, *736*, 119. [CrossRef]
15. Seon, K.-I.; Edelstein, J.; Korpela, E.; Witt, A.; Min, K.W.; Han, W.; Shinn, J.; Kim, I.J.; Park, J.W. Observation of the Far-Ultraviolet Continuum Background with SPEAR/FIMS. *Astrophys. J. Suppl. Ser.* **2011**, *196*, 15. [CrossRef]
16. Chellew, B.; Brandt, T.D.; Hensley, B.S.; Draine, B.T.; Matthaey, E. An Optical Spectrum of the Diffuse Galactic Light from BOSS and IRIS. *Astrophys. J.* **2022**, *932*, 112. [CrossRef]
17. Madau, P.; Pozzetti, L. Deep galaxy counts, extragalactic background light and the stellar baryon budget. *Mon. Not. R. Astron. Soc.* **2000**, *312*, L9–L15. [CrossRef]
18. Marsden, G.; Ade, P.A.R.; Bock, J.J.; Chapin, E.L.; Devlin, M.J.; Dicker, S.R.; Griffin, M.; Gundersen, J.O.; Halpern, M.; Hargrave, P.C.; et al. BLAST: Resolving the Cosmic Submillimeter Background. *Astrophys. J.* **2009**, *707*, 1729. [CrossRef]
19. Koushan, S.; Driver, S.P.; Bellstedt, S.; Davies, L.J.; Robotham, A.S.G.; del P. Lagos, C.; Hashemizadeh, A.; Obreschkow, D.; Thorne, J.E.; Bremer, M.; et al. GAMA/DEVILS: Constraining the cosmic star formation history from improved measurements of the 0.3–2.2 μm extragalactic background light. *Mon. Not. R. Astron. Soc.* **2021**, *503*, 2033. [CrossRef]
20. Stecker, F.W.; de Jager, O.C.; Salamon, M.H. TeV Gamma Rays from 3C 279: A Possible Probe of Origin and Intergalactic Infrared Radiation Fields. *Astrophys. J. Lett.* **1992**, *390*, L49. [CrossRef]
21. Nikishov, A.I. Absorption of High-Energy Photons in the Universe. *Sov. Phys.—JETP* **1962**, *14*, 393.

22. Gould, R.J.; Schréder, G. Opacity of the Universe to High-Energy Photons. *Phys. Rev. Lett.* **1966**, *16*, 252. [CrossRef]
23. Ajello, M.; Baldini, L.; Ballet, J.; Bastieri, D.; Becerra Gonzalez, J.; Bellazzini, R.; Berretta, A.; Bissaldi, E.; Bonino, R.; Brill, A.; et al. The Fourth Catalog of Active Galactic Nuclei Detected by the Fermi Large Area Telescope. *Astrophys. J.* **2020**, *892*, 105. [CrossRef]
24. Abdollahi, S.; Ajello, M.; Baldini, L.; Ballet, J. Incremental Fermi Large Area Telescope Fourth Source Catalog. *Astrophys. J. Suppl. Ser.* **2022**, *260*, 53. [CrossRef]
25. Wills, B.J.; Thompson, K.L.; Han, M.; Netzer, H.; Wills, D.; Baldwin, J.A.; Ferland, G.J.; Browne, I.W.A.; Brotherton, M.S. Hubble Space Telescope Sample of Radio-loud Quasars: Ultraviolet Spectra of the First 31 Quasars. *Astrophys. J.* **1995**, *447*, 139. [CrossRef]
26. Adelman-McCarthy, J.K.; Agüeros, M.A.; Allam, S.S.; Prieto, C.A.; Anderson, K.S.J.; Anderson, S.F.; Annis, J.; Bahcall, N.A.; Bailer-Jones, C.A.L.; Baldry, I.K.; et al. The Sixth Data Release of the Sloan Digital Sky Survey. *Astrophys. J. Suppl. Ser.* **2008**, *175*, 297. [CrossRef]
27. Pâris, I.; Petitjean, P.; Aubourg, É.; Myers, A.D. The Sloan Digital Sky Survey Quasar Catalog: Fourteenth data release. *Astron. Astrophys.* **2018**, *613*, A51. [CrossRef]
28. Rossetti, A.; Mantovani, F.; Dallacasa, D.; Fanti, C.; Fanti, R. Multi-frequency VLBA observations of compact sources from the Peacock and Wall catalogue. *Astron. Astrophys.* **2005**, *434*, 449. [CrossRef]
29. McConville, W.; Ostorero, L.; Moderski, R.; Stawarz, L.; Cheung, C.C.; Ajello, M.; Bouvier, A.; Bregeon, J.; Donato, D.; Finke, J.; et al. Fermi Large Area Telescope Observations of the Active Galaxy 4C +55.17: Steady, Hard Gamma-Ray Emission and Its Implications. *Astrophys. J.* **2011**, *738*, 148. [CrossRef]
30. Taylor, G.B.; Healey, S.E.; Helmboldt, J.F.; Tremblay, S.; Fassnacht, C.D. Characteristics of EGRET Blazars in the VLBA Imaging and Polarimetry Survey (VIPS). *Astrophys. J.* **2007**, *671*, 1355. [CrossRef]
31. O'Dea, C.P. The Compact Steep-Spectrum Radio Sources. *Publ. Astron. Soc. Pac.* **1998**, *110*, 493. [CrossRef]
32. Hartman, R.C.; Bertsch, D.L.; Bloom, S.D.; Chen, A.W.; Deines-Jones, P.; Esposito, J.A.; Fichtel, C.E.; Friedlander, D.P.; Hunter, S.D.; McDonald, L.M.; et al. The Third EGRET Catalog of High-Energy Gamma-Ray Sources. *Astrophys. J. Suppl. Ser.* **1999**, *123*, 79. [CrossRef]
33. Mukherjee, R. EGRET gamma-ray sources: Observations and physics. *Bull. Astron. Soc. India* **2002**, *30*, 73.
34. Atwood, W.B.; Abdo, A.A.; Ackermann, M.; Althouse, W.T.; Anderson, B.; Axelsson, M.; Baldini, L.; Ballet, J.; Band, D.L.; Barbiellini, G.; et al. The Large Area Telescope on the Fermi Gamma-Ray Space Telescope Mission. *Astrophys. J.* **2009**, *697*, 1071. [CrossRef]
35. Abdollahi, S.; Acero, F.; Ackermann, M.; Ajello, M.; Atwood, W.B.; Axelsson, M.; Baldini, L.; Ballet, J.; Barbiellini, G.; Bastieri, D.; et al. Fermi Large Area Telescope Fourth Source Catalog. *Astrophys. J. Suppl. Ser.* **2020**, *247*, 53. [CrossRef]
36. Abdo, A.A.; Ackermann, M.; Ajello, M. The First Catalog of Active Galactic Nuclei Detected by the Fermi Large Area Telescope. *Astrophys. J.* **2010**, *715*, 429. [CrossRef]
37. Nolan, P.L.; Abdo, A.A.; Ackermann, M.; Ajello, M.; Allafort, A.; Antolini, E.; Atwood, W.B.; Axelsson, M.; Baldini, L.; Ballet, J.; et al. Fermi Large Area Telescope Second Source Catalog. *Astrophys. J.* **2012**, *199*, 31. [CrossRef]
38. Nikolsky, S.I.; Sinitsyna, V.G. Investigation of gamma-sources by mirror telescope. In *Proceedings of the International Workshop of Very Hight Energy Gamma-Ray Astronomy, Crimea, USSR, 17–21 April 1989*; Stepanian, A.A., Fegan, D.J., Cawley, W.F., Eds.; Physics Department University College Dublin: Dublin, Ireland, 1989; p. 11.
39. Sinitsyna, V.G. Searches for gamma-quanta from local sources by a wide-angle imaging telescope. *Nuovo Cim. C* **1996**, *19*, 965. [CrossRef]
40. Sinitsyna, V.G.; Sinitsyna, V.Y.; Borisov, S.S.; Klimov, A.I.; Mirzafatikhov, R.M.; Moseiko, N.I. Very high energy astrophysics with the SHALON Cherenkov telescopes. *Nucl. Instrum. Methods Phys. Res. A* **2020**, *952*, 161775. [CrossRef]
41. Sinitsyna, V.G.; Alaverdyan, A.Y.; Andreeva, M.S.; Balygin, K.A.; Borisov, S.S.; Ivanov, I.A.; Kirichenko, A.M.; Klimov, A.I.; Kozhukhova, I.P.; Mirzafatikhov, R.M.; et al. SHALON observations of Active Galactic Nuclei at red shift from z = 0.0179 to z = 1.375. In *Proceedings of "Astroparticle, Particle, Space Physics and Detectors Physics Applications"*; Giani, S., Leroy, C., Rancoita, P.-G., Price, L., Ruchti, R., Eds.; World Scientific: Singapore, 2014; Volume 8, p. 20.
42. Li, T.-P.; Ma, Y.-Q. Analysis methods for results in gamma-ray astronomy. *Astrophys. J.* **1983**, *272*, 317. [CrossRef]
43. Sinitsyna, V.G.; Sinitsyna, V.Y. Investigations of the active galactic nucleus 4C +55.17 at high and very-high energies. *Astron. Nachrichten* 2026, *in print*.
44. Stecker, F.W.; Malkan, M.A.; Scully, S.T. Intergalactic photon spectra from the far—IR to the UV Lyman limit for 0 < z < 6 and the optical depth of the universe to high—Energy gamma rays. *Astrophys. J.* **2006**, *648*, 774.
45. Kneiske, T.M.; Bretz, T.; Mannheim, K.; Hartmann, D.H. Implications of cosmological gamma-ray absorption. II. Modification of gamma-ray spectra. *Astron. Astrophys.* **2004**, *413*, 807. [CrossRef]
46. Stecker, F.W.; Malkan, M.A.; Scully, S.T. An Empirical Determination of the Intergalactic Background Light from UV to FIR Wavelengths Using FIR Deep Galaxy Surveys and the Gamma-Ray Opacity of the Universe. *Astrophys. J.* **2016**, *827*, 6. [CrossRef]
47. Kneiske, T.M.; Mannheim, K.; Hartmann, D.H. Implications of cosmological gamma-ray absorption I. Evolution of the metagalactic radiation field. *Astron. Astrophys.* **2002**, *386*, 1. [CrossRef]

48. Kneiske, T.M.; Dole, H. A lower-limit flux for the extragalactic background light. *Astron. Astrophys.* **2010**, *515*, A19. [CrossRef]
49. Finke, J.D.; Razzaque, S.; Dermer, C.D. Modeling the extragalactic background light from stars and dust. *Astrophys. J.* **2010**, *712*, 238. [CrossRef]
50. Franceschini, A.; Rodighiero, G.; Vaccari, M. Extragalactic optical-infrared background radiation, its time evolution and the cosmic photon-photon opacity. *Astron. Astrophys.* **2008**, *487*, 837. [CrossRef]
51. Peebles, P.J.E. *Principles of Physical Cosmology*; Princeton University Press: Princeton, NJ, USA, 1993.
52. Ackermann, M.; Ajello, M.; Allafort, A.; Schady, P.; Baldini, L.; Ballet, J.; Barbiellini, G.; Bastieri, D.; Bellazzini, R.; Blandford, R.D.; et al. The Imprint of the Extragalactic Background Light in the Gamma-Ray Spectra of Blazars. *Science* **2012**, *338*, 1190. [CrossRef]
53. Abdollahi, S. et al. [Fermi-LAT Collaboration] A gamma-ray determination of the Universe's star formation history. *Science* **2018**, *362*, 1031. [CrossRef]
54. Biteau, J.; Williams, D.A. The Extragalactic Background Light, the Hubble Constant, and Anomalies: Conclusions from 20 Years of TeV Gamma-ray Observations. *Astrophys. J.* **2015**, *812*, 60. [CrossRef]
55. Sinitsyna, V.G.; Sinitsyna, V.Y.; Borisov, S.S.; Mirzafatikhov, R.M.; Balygin, K.A.; Klimov, A.I.; Ostashev, I.E.; Moseiko, N.I. Probing of extragalactic background light with TeV gamma-ray observations. *Astron. Nachrichten* **2021**, *347*, 438. [CrossRef]
56. Finke, J.D.; Ajello, M.; Dominguez, A.; Desai, A. Modeling the Extragalactic Background Light and the Cosmic Star Formation History. *Astrophys. J.* **2022**, *941*, 33. [CrossRef]

Disclaimer/Publisher's Note: The statements, opinions and data contained in all publications are solely those of the individual author(s) and contributor(s) and not of MDPI and/or the editor(s). MDPI and/or the editor(s) disclaim responsibility for any injury to people or property resulting from any ideas, methods, instructions or products referred to in the content.